Oceanic Internal Wave Field: Theory of Scale-invariant Spectra

Yuri V. Lvov

Department of Mathematical Sciences, Rensselaer Polytechnic Institute, Troy, New York 12180 USA

Kurt L. Polzin

Woods Hole Oceanographic Institution, MS#21, Woods Hole, MA 02543 USA

Esteban G. Tabak

Courant Institute of Mathematical Sciences, New York University, New York, NY 10012 USA

Naoto Yokoyama

Department of Mechanical Engineering, Doshisha University, Kyotanabe, Kyoto 610-0394 Japan
(Dated: July 10, 2008)

Steady scale-invariant solutions of a kinetic equation describing the statistics of oceanic internal gravity waves based on wave turbulence theory are investigated. It is shown that the scale-invariant collision integral in the kinetic equation diverges for almost all spectral power-law exponents. These divergences come from resonant interactions with infra-red and/or ultra-violet wavenumbers with extreme scale-separations.

We identify a small domain in which the scale-invariant collision integral converges and numerically find a convergent power-law solution. This numerical solution is close to the Garrett–Munk spectrum. Power-law exponents which potentially permit a balance between the infra-red and ultra-violet divergences are also discussed. The balanced exponents are generalizations of an exact solution of the scale-invariant kinetic equation, the Pelinovsky–Raevsky spectrum.

Ways to regularize this divergence are considered. A small but finite Coriolis parameter representing the effects of rotation is introduced into the kinetic equation to determine solutions over the divergent part of the domain using rigorous asymptotic arguments. This gives rise to the induced diffusion regime.

The derivation of the kinetic equation is based on an assumption of weak nonlinearity. Dominance of the nonlocal interactions puts the self-consistency of the kinetic equation at risk. Yet these weakly nonlinear stationary states are consistent with much of the observational evidence.

I. INTRODUCTION

Wave-wave interactions in continuously stratified flows have been a subject of intensive research in the last few decades. Of particular importance is the observation of a nearly universal internal-wave energy spectrum in the ocean, first described by Garrett and Munk. It is generally thought that the existence of a universal spectrum is at least partly the result of nonlinear interactions among internal waves. Due to the quadratic nonlinearity of the underlying fluid equations and dispersion relation allowing three-wave resonances, internal waves interact through triads. In the weakly nonlinear regime, the nonlinear interactions among internal waves concentrate on their *resonant* set, and can be described by a kinetic equation, which assumes the familiar form[1,2,3,4,5,6,7,8,9,10,11,12,13,14]:

$$
\begin{aligned}
\frac{\partial n_{\boldsymbol{p}}}{\partial t} = 4\pi \int d\boldsymbol{p}_{12} \, \big(&|V_{\boldsymbol{p}_1,\boldsymbol{p}_2}^{\boldsymbol{p}}|^2 \, f_{\boldsymbol{p}_1 \boldsymbol{p}_2}^{\boldsymbol{p}} \, \delta_{\boldsymbol{p}-\boldsymbol{p}_1-\boldsymbol{p}_2} \, \delta_{\omega_{\boldsymbol{p}}-\omega_{\boldsymbol{p}_1}-\omega_{\boldsymbol{p}_2}} \\
&- |V_{\boldsymbol{p}_2,\boldsymbol{p}}^{\boldsymbol{p}_1}|^2 \, f_{\boldsymbol{p}_2 \boldsymbol{p}}^{\boldsymbol{p}_1} \, \delta_{\boldsymbol{p}_1-\boldsymbol{p}_2-\boldsymbol{p}} \, \delta_{\omega_{\boldsymbol{p}_1}-\omega_{\boldsymbol{p}_2}-\omega_{\boldsymbol{p}}} \\
&- |V_{\boldsymbol{p},\boldsymbol{p}_1}^{\boldsymbol{p}_2}|^2 \, f_{\boldsymbol{p}\boldsymbol{p}_1}^{\boldsymbol{p}_2} \, \delta_{\boldsymbol{p}_2-\boldsymbol{p}-\boldsymbol{p}_1} \, \delta_{\omega_{\boldsymbol{p}_2}-\omega_{\boldsymbol{p}}-\omega_{\boldsymbol{p}_1}} \big) , \\
\text{with} \quad &f_{\boldsymbol{p}_1 \boldsymbol{p}_2}^{\boldsymbol{p}} = n_{\boldsymbol{p}_1} n_{\boldsymbol{p}_2} - n_{\boldsymbol{p}} (n_{\boldsymbol{p}_1} + n_{\boldsymbol{p}_2}) .
\end{aligned}
\tag{1}
$$

Here $n_{\boldsymbol{p}} = n(\boldsymbol{p})$ is a three-dimensional action spectrum (see Eq. (16)) with wavenumber $\boldsymbol{p} = (\boldsymbol{k}, m)$, i.e. $\boldsymbol{k}$ and m are the horizontal and vertical components of $\boldsymbol{p}$. The frequency ω is given by a linear dispersion relation. The wavenumbers are signed variables, while the wave frequencies are always positive. The factor $V_{\boldsymbol{p}_1 \boldsymbol{p}_2}^{\boldsymbol{p}}$ is the interaction matrix describing the transfer of wave action among the members of a resonant triad.

Following Kolmogorov's viewpoint of energy cascades in isotropic Navier–Stokes turbulence, one may look for statistically stationary states using scale-invariant solutions to the kinetic equation (1). The solution may occur in an inertial subrange of wavenumbers and frequencies that are far from those where forcing and dissipation act, and also

far from characteristic scales of the system, including the Coriolis frequency resulting from the rotation of the Earth, the buoyancy frequency due to stratification and the ocean depth. Under these assumptions, the dispersion relation and the interaction matrix elements are locally scale-invariant. It is natural, therefore, in this restricted domain, to look for self-similar solutions of Eq. (1), which take the form

$$n(\boldsymbol{k}, m) = |\boldsymbol{k}|^{-a}|m|^{-b}. \tag{2}$$

Values of a and b in the right-hand side of Eq. (1) vanishes identically correspond to steady solutions of the kinetic equation, and hopefully also to statistically steady states of the ocean's wave field. Unlike Kolmogorov turbulence, the exponents which give steady solutions can not be determined by the dimensional analysis alone (see, for example, Ref. 15). This is the case owing to multiple characteristic length scales in anisotropic systems.

Before seeking steady solutions, however, one should find out whether the improper integrals in the kinetic equation (1) converge. This is related to the question of *locality* of the interactions: a convergent integral characterizes the physical scenario where interactions of neighboring wavenumbers dominate the evolution of the wave spectrum, while a divergent one implies that distant, nonlocal interactions in the wavenumber space dominate.

It turns out that the internal-wave collision integral diverges for *almost* all values of a and b. In particular, the collision integral has an infra-red (IR) divergence at zero, i.e. $|\boldsymbol{k}_1|$ or $|\boldsymbol{k}_2| \to 0$ and an ultra-violet (UV) divergence at infinity, i.e. $|\boldsymbol{k}_1|$ and $|\boldsymbol{k}_2| \to \infty$. There is only one exception where the integral converges: the segment with $b = 0$ and $7/2 < a < 4$. This segment corresponds to wave action independent of vertical wavenumbers, $\partial n/\partial m = 0$. Within this segment we numerically determine a new steady *convergent* solution to Eq. (1), with

$$n(\boldsymbol{k}, m) \propto |\boldsymbol{k}|^{-3.7}. \tag{3}$$

This solution is not far from the large-wavenumber form of the Garrett–Munk (GM) spectrum:

$$n(\boldsymbol{k}, m) \propto |\boldsymbol{k}|^{-4} . \tag{4}$$

Alternatively, one can explore the physical interpretation of divergent solutions. We find a region in (a, b) space where there are both IR and UV divergences having opposite signs. This suggests a possible scenario where the two divergent contributions may cancel each other, yielding a steady state. An example of such a case is provided by the Pelinovsky–Raevsky (PR) spectrum,

$$n_{\boldsymbol{k}, m} \propto |\boldsymbol{k}|^{-7/2}|m|^{-1/2}. \tag{5}$$

This solution, however, is only one among infinitely many. The problem at hand is a generalization of the concept of principal value integrals: for a and b which give opposite signs of the divergences at zero and infinity, one can *regularize* the integral by cutting out small neighborhoods of the two singularities in such a way that the divergences cancel each other and the remaining contributions are small. Hence all the exponents which yield opposite-signed divergence at the both ends can be steady solutions of Eq. (1). As we will see below this general statement helps to describe the experimental oceanographic data which are available to us. The nature of such steady solutions depends on the particular truncation of the divergent integrals.

So far, we have kept the formalism at the level of the self-similar limit of the kinetic equation (1). However, once one considers energy transfer mechanisms dominated by interactions with extreme modes of the system, one can no longer neglect the deviations from self-similarity near the spectral boundaries: the inertial frequency due to the rotation of the Earth at the IR end, and the buoyancy frequency and/or dissipative cut-offs at the UV end.

For example, we may consider a scenario in which interactions with the smallest horizontal wavenumbers dominate the energy transfer within the inertial subrange, either because the collision integral at infinity converges or because the system is more heavily truncated at the large wavenumbers by wave breaking or dissipation. We will demonstrate that the IR divergence of the collision integral has a simple physical interpretation: the evolution of each wave is dominated by the interaction with its nearest neighboring vertical wavenumbers, mediated by the smallest horizontal wavenumbers of the system, a mechanism denoted Induced Diffusion in the oceanographic literature.

To bring back the effects of the rotation of the Earth in Eq. (1), one introduces the Coriolis parameter f there and in the linear dispersion relation. Since we are considering the evolution of waves with frequency ω much larger than f, f can be considered to be small. However, since the interaction with waves near f dominates the energy transfer, one needs to invert the order in which the limits are taken, postponing making f zero to the end. This gives rise to an integral that diverges like f raised to a negative power smaller than -1, but multiplied by a prefactor that vanishes if either $9 - 2a - 3b = 0$ or $b = 0$. These are the induced diffusion lines of steady state solutions, found originally in Ref. 16. This family of stationary states does a reasonable job of explaining the gamut of observed variability.

The paper is organized as follows. Wave turbulence theory for the internal wave field and the corresponding kinetic equation are briefly summarized in Sec. II along with the motivating observations. We analyze the divergence of the

kinetic equation in Sec. III. Section IV includes a special, convergent power-law solution that may account for the GM spectrum. In Sec. V we introduce possible quasi-steady solutions of the kinetic equation which are based on cancellations of two singularities. Section VI shows that the IR divergence is dominated by induced diffusion, and computes the family of power-law solutions which arises from taking it into account. We conclude in Sec. VII.

II. WAVE TURBULENCE THEORY FOR INTERNAL WAVES

A. Background and history

The idea of using wave turbulence formalism to describe internal waves is certainly not new; it dates to Kenyon, with calculations of the kinetic equations for oceanic spectra presented in Refs. 6,10,12.

Various formulations have been developed for characterizing wave-wave interactions in the stratified wave turbulence in the last four decades (see Ref. 17 for a brief review, and Refs. 1,2,3,4,5,6,7,8,9,10,11,12,13 for details).

We briefly discuss the derivation of the kinetic equation and wave-wave interaction matrix elements below in Eq. (15).

The starting point for the most extensive investigations has been a non-canonical Hamiltonian formulation in Lagrangian coordinates[16] that requires an unconstrained approximation in smallness of wave amplitude in addition to the assumption that nonlinear transfers take place on much longer time scales than the underlying linear dynamics. Other work has as its basis a formulation in Clebsh-like variables[11] and a non-Hamiltonian formulation in Eulerian coordinates[1]. Here we employ a canonical Hamiltonian representation in isopycnal coordinates[5] which, as a canonical representation, preserves the original symmetries and hence conservation properties of the original equations of motion.

Energy transfers in the kinetic equation are characterized by three simple mechanisms identified by Ref. 6 and reviewed by Ref. 18. These mechanisms represent extreme scale-separated limits. One of these mechanisms represents the interaction of two small vertical scale, high frequency waves with a large vertical scale, near-inertial (frequency near f) wave and has received the name Induced Diffusion (ID). The ID mechanism exhibits a family of stationary states, i.e. a family of solutions to Eq. (2). A comprehensive inertial-range theory with constant downscale transfer of energy can be obtained by patching these mechanisms together in a solution that closely mimics the empirical universal spectrum (GM). A fundamental caveat from this work is that the interaction time scales of high frequency waves are sufficiently small at small spatial scales as to violate the assumption of weak nonlinearity.

In parallel work, Pelinovsky and Raevsky[11] derived a kinetic equation for oceanic internal waves. They also have found the statistically steady state spectrum of internal waves, Eq. (5), which we propose to call Pelinovsky-Raevsky spectrum. This spectrum was latter found in Refs. 1,5. It follows from applying the Zakharov–Kuznetsov conformal transformation, which effectively establishes a map between the neighborhoods of zero and infinity. Making these two contributions cancel point-wisely yields the solution (5).

Both Pelinovsky and Raevsky[11] and Caillol and Zeitlin[1] noted that the solution (5) comes through a cancellation between oppositely signed divergent contributions in their respective collision integrals. A fundamental caveat is that one can not use conformal mapping for divergent integrals. Therefore, the existence of such a solution is fortuitous.

Here we demonstrate that our canonical Hamiltonian structure admits to a similar characterization: power-law solutions of the form (2) return collision integrals that are, in general, divergent. Regularization of the integral allows us to examine the conditions under which it is possible to rigorously determine the power-law exponents (a, b) in Eq. (2) that lead to stationary states. In doing so we obtain the ID family.

The situation is somewhat peculiar: We have assumed weak nonlinearity to derive the kinetic equation. The kinetic equation then predicts that nonlocal, strongly scale-separated interactions dominate the dynamics. These interactions have a less chance to be weakly nonlinear than regular, "local" interactions. Thus the derivation of the kinetic equation and its self-consistency is at risk. As we will see below, despite this caveat, the weakly nonlinear theory is consistent with much of the observational evidence.

B. Experimental motivation

Power laws provide a simple and intuitive physical description of complicated wave fields. Therefore we assumed that the spectral energy density can be represented as Eq. (2), and undertook a systematic study of published observational programs. In doing so we were fitting the experimental data available to us by power-law spectra. We were presuming that the power laws offer a good fit of the data. We were not assuming that spectra are given by Garrett and Munk spectrum. That effort is reported in detail on elsewhere[19], here we just give a brief synopsis to motivate present theoretical study.
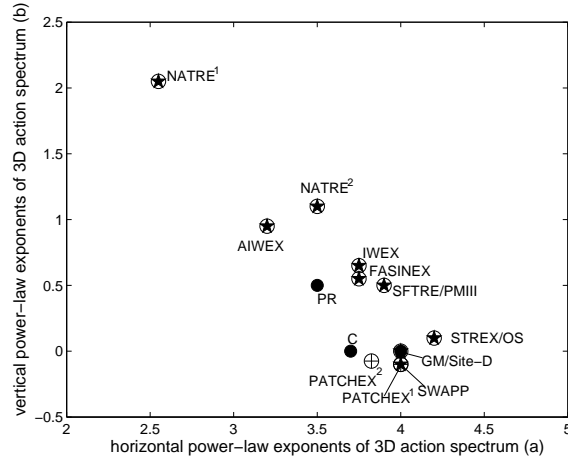
We reviewed the following observational programs:

FIG. 1: The observational points. The filled circles represent the Pelinovsky–Raevsky (PR) spectrum, the convergent numerical solution determined in Sec. IV (C) and the GM spectrum. Circles with stars represent estimates based upon one-dimensional spectra from the western North Atlantic south of the Gulf Stream (IWEX, FASINEX and SFTRE/PMIII), the eastern North Pacific (STREX/OS and PATCHEX[1]), the western North Atlantic north of the Gulf Stream (Site-D), the Arctic (AIWEX) and the eastern North Atlantic (NATRE[1] and NATRE[2]). There are two estimates obtained from two-dimensional data sets from the eastern North Pacific (SWAPP and PATCHEX[2]) represented as circles with cross hairs. NATRE[1] represents a fit over frequencies of $1 < \omega < 6\text{cpd}$ and NATRE[2] a fit over higher frequencies.

- The Internal Wave Experiment (IWEX)[20];

- The Arctic Internal Wave Experiment (AIWEX)[21,22];

- The Frontal Air-Sea Interaction Experiment (FASINEX)[23,24];

- The Patches Experiment (PATCHEX)[25];

- The Surface Wave Process Program (SWAPP) experiment[26];

- North Atlantic Tracer Release Experiment (NATRE)[27] / Subduction[28];

- Salt Finger Tracer Release Experiment (SFTRE)[29] / Polymode IIIc (PMIII)[30];

- Site-D[31];

- Storm Transfer and Response Experiment (STREX)[32] / Ocean Storms Experiment (OS)[33].

Here we extract the summary of that study in the form of Fig. 1, in which estimates of power-law exponents (a, b) are plotted against each other.

That study comes with many caveats. The most important here is that the power-law exponents, (a, b), are not typically derived from two-dimensional horizontal wavenumber, vertical wavenumber spectra. The power laws were fit to one-dimensional frequency and one-dimensional vertical wavenumber spectra of energy, $e(\omega) \propto \omega^{-c}$ and $e(m) \propto m^{-d}$, with conversion to (a, b) requiring that:

$$a = c + 2 \quad \text{and} \quad b = d - c.$$

This procedure explicitly assumes that the two-dimensional spectra are separable. That is to say that the ω–m spectrum can be represented as a product of function of ω and function of m alone. It is clear that this assumption is not warranted in all cases. This is particularly true of the NATRE data, for which two power-law estimates are provided. Nevertheless, this is the best data that is available to us at a present time. We see that these points are not randomly scattered, but have some pattern. Explaining the location of the experimental points and making sense out of this pattern is the main physical motivation for this study.

C. Hamiltonian Structure and Wave Turbulence Theory

This subsection briefly summarizes the derivation in Ref. 5; it is included here only for completeness and to allow references from the core of the paper.

The equations of motion satisfied by an incompressible stratified rotating flow in hydrostatic balance under the Boussinesq approximation are:

$$
\begin{aligned}
\frac{\partial}{\partial t}\frac{\partial z}{\partial \rho} + \nabla \cdot \left(\frac{\partial z}{\partial \rho}\boldsymbol{u}\right) &= 0, \\
\frac{\partial \boldsymbol{u}}{\partial t} + f\boldsymbol{u}^\perp + \boldsymbol{u}\cdot\nabla\boldsymbol{u} + \frac{\nabla M}{\rho_0} &= 0, \\
\frac{\partial M}{\partial \rho} - gz &= 0.
\end{aligned}
\tag{6}
$$

These equations result from mass convervation, horizontal momentum convervation and hydrostatic balance. The equations are written in isopycnal coordinates with the density ρ replacing the height z in its role as independent vertical variable. Here $\boldsymbol{u} = (u, v)$ is the horizontal component of the velocity field, $\boldsymbol{u}^\perp = (-v, u)$, $\nabla = (\partial/\partial x, \partial/\partial y)$ is the gradient operator along isopycnals, M is the Montgomery potential

$$
M = P + g\,\rho\,z\,,
$$

f is the Coriolis parameter, and ρ_0 is a reference density in its role as inertia, considered constant under the Boussinesq approximation.

The potential vorticity is given by

$$
q = \frac{f + \partial v/\partial y - \partial u/\partial x}{\Pi},
\tag{7}
$$

where $\Pi = \rho/g\partial^2 M/\partial\rho^2 = \rho\partial z/\partial\rho$ is a normalized differential layer thickness. Since both the potential vorticity and the fluid density are conserved along particle trajectories, an initial profile of the potential vorticity that is a function of the density will be preserved by the flow. Hence it is self-consistent to assume that

$$
q(\rho) = q_0(\rho) = \frac{f}{\Pi_0(\rho)},
\tag{8}
$$

where $\Pi_0(\rho) = -g/N(\rho)^2$ is a reference stratification profile with the constant background buoyancy frequency, $N = (-g/(\rho\partial z/\partial\rho|_{\text{bg}}))^{1/2}$. This assumption is not unrealistic: it represents a pancake-like distribution of potential vorticity, the result of its comparatively faster homogenization along than across isopycnal surfaces.

It is shown in Ref. 5 that the primitive equations of motion (6) under the assumption (8) can be written as a pair of canonical Hamiltonian equations,

$$
\frac{\partial \Pi}{\partial t} = -\frac{\delta \mathcal{H}}{\delta \phi}, \qquad \frac{\partial \phi}{\partial t} = \frac{\delta \mathcal{H}}{\delta \Pi},
\tag{9}
$$

where ϕ is the isopycnal velocity potential, and the Hamiltonian is the sum of kinetic and potential energies,

$$
\mathcal{H} = \int d\boldsymbol{x}d\rho \left(-\frac{1}{2}\left(\Pi_0 + \Pi(\boldsymbol{x}, \rho)\right) \left| \nabla\phi(\boldsymbol{x}, \rho) + \frac{f}{\Pi_0}\nabla^\perp\Delta^{-1}\Pi(\boldsymbol{x}, \rho) \right|^2 + \frac{g}{2}\left| \int^\rho d\rho' \frac{\Pi(\boldsymbol{x}, \rho')}{\rho'} \right|^2 \right).
\tag{10}
$$

Here, $\nabla^\perp = (-\partial/\partial y, \partial/\partial x)$ and Δ^{-1} is the inverse Laplacian.

Switching to Fourier space, and introducing a complex field variable $a_{\boldsymbol{p}}$ through the transformation

$$
\begin{aligned}
\phi_{\boldsymbol{p}} &= \frac{iN\sqrt{\omega_{\boldsymbol{p}}}}{\sqrt{2g}|\boldsymbol{k}|}\left(a_{\boldsymbol{p}} - a^*_{-\boldsymbol{p}}\right), \\
\Pi_{\boldsymbol{p}} &= \Pi_0 - \frac{N\Pi_0|\boldsymbol{k}|}{\sqrt{2\,g\omega_{\boldsymbol{p}}}}\left(a_{\boldsymbol{p}} + a^*_{-\boldsymbol{p}}\right),
\end{aligned}
\tag{11}
$$

where the frequency ω satisfies the linear dispersion relation

$$\omega_{\boldsymbol{p}} = \sqrt{f^2 + \frac{g^2}{\rho_0^2 N^2}\frac{|\boldsymbol{k}|^2}{m^2}}, \tag{12}$$

the equations of motion (6) adopt the canonical form

$$i\frac{\partial}{\partial t}a_{\boldsymbol{p}} = \frac{\delta\mathcal{H}}{\delta a_{\boldsymbol{p}}^*}, \tag{13}$$

with Hamiltonian:

$$\begin{aligned}
\mathcal{H} = &\int d\boldsymbol{p}\,\omega_{\boldsymbol{p}}|a_{\boldsymbol{p}}|^2 \\
&+\int d\boldsymbol{p}_{012}\left(\delta_{\boldsymbol{p}+\boldsymbol{p}_1+\boldsymbol{p}_2}(U_{\boldsymbol{p},\boldsymbol{p}_1,\boldsymbol{p}_2}a_{\boldsymbol{p}}^*a_{\boldsymbol{p}_1}^*a_{\boldsymbol{p}_2}^* + \text{c.c.})\right. \\
&\left.+\delta_{-\boldsymbol{p}+\boldsymbol{p}_1+\boldsymbol{p}_2}(V_{\boldsymbol{p}_1,\boldsymbol{p}_2}^{\boldsymbol{p}}a_{\boldsymbol{p}}^*a_{\boldsymbol{p}_1}a_{\boldsymbol{p}_2} + \text{c.c.})\right).
\end{aligned} \tag{14}$$

This is the standard form of the Hamiltonian of a system dominated by three-wave interactions[14]. Calculations of interaction coefficients are tedious but straightforward task, completed in Ref. 5. These coefficients are given by

$$V_{\boldsymbol{p}_1,\boldsymbol{p}_2}^{\boldsymbol{p}} = \frac{N}{4\sqrt{2g}}\frac{1}{kk_1k_2}\left(I_{\boldsymbol{p},\boldsymbol{p}_1,\boldsymbol{p}_2} + J_{\boldsymbol{p}_1,\boldsymbol{p}_2}^{\boldsymbol{p}} + K_{\boldsymbol{p},\boldsymbol{p}_1,\boldsymbol{p}_2}\right), \tag{15a}$$

$$U_{\boldsymbol{p},\boldsymbol{p}_1,\boldsymbol{p}_2} = \frac{N}{4\sqrt{2g}}\frac{1}{3}\frac{1}{kk_1k_2}\left(I_{\boldsymbol{p},\boldsymbol{p}_1,\boldsymbol{p}_2} + J_{\boldsymbol{p}_1,\boldsymbol{p}_2}^{-\boldsymbol{p}} + K_{\boldsymbol{p},\boldsymbol{p}_1,\boldsymbol{p}_2}\right), \tag{15b}$$

$$\begin{aligned}
I_{\boldsymbol{p},\boldsymbol{p}_1,\boldsymbol{p}_2} = &-\sqrt{\frac{\omega_1\omega_2}{\omega}}k^2\boldsymbol{k}_1\cdot\boldsymbol{k}_2 \\
&-((0,1,2)\to(1,2,0))-((0,1,2)\to(2,0,1)),
\end{aligned} \tag{15c}$$

$$\begin{aligned}
J_{\boldsymbol{p}_1,\boldsymbol{p}_2}^{\boldsymbol{p}} = &\frac{f^2}{\sqrt{\omega\omega_1\omega_2}}\big(k^2\boldsymbol{k}_1\cdot\boldsymbol{k}_2 \\
&-((0,1,2)\to(1,2,0))-((0,1,2)\to(2,0,1))\big),
\end{aligned} \tag{15d}$$

$$\begin{aligned}
K_{\boldsymbol{p},\boldsymbol{p}_1,\boldsymbol{p}_2} = &-if\left(\left(\sqrt{\frac{\omega}{\omega_1\omega_2}}(k_1^2-k_2^2)\boldsymbol{k}_1\cdot\boldsymbol{k}_2^{\perp}\right.\right. \\
&\left.\left.+\big((0,1,2)\to(1,2,0)\big)+\big((0,1,2)\to(2,0,1)\big)\right)\right),
\end{aligned} \tag{15e}$$

where $((0,1,2)\to(1,2,0))$ and $((0,1,2)\to(2,0,1))$ denote exchanges of suffixes. We stress that the field equation (13) with the three-wave Hamiltonian (12, 14, 15) is *equivalent* to the primitive equations of motion for internal waves (6). Other approaches, in particular the Lagrangian approach, is based on small-amplitude expansion to arrive to this type of equations.

In wave turbulence theory, one proposes a perturbation expansion in the amplitude of the nonlinearity, yielding linear waves at the leading order. Wave amplitudes are modulated by the nonlinear interactions, and the modulation is statistically described by an kinetic equation[14] for the wave action $n_{\boldsymbol{p}}$ defined by

$$n_{\boldsymbol{p}}\delta(\boldsymbol{p}-\boldsymbol{p}') = \langle a_{\boldsymbol{p}}^*a_{\boldsymbol{p}'}\rangle. \tag{16}$$

The derivation of this kinetic equation is well studied and understood. For the three-wave Hamiltonian (14), the kinetic equation is the one in Eq. (1), describing general internal waves interacting in both rotating and non-rotating environments.

The delta functions in the kinetic equation ensures that spectral transfer happens on the *resonant manifold*, defined

as

$$\begin{cases} \boldsymbol{p} = \boldsymbol{p}_1 + \boldsymbol{p}_2 \\ \omega = \omega_1 + \omega_2 \end{cases} , \tag{17a}$$

$$\begin{cases} \boldsymbol{p}_1 = \boldsymbol{p}_2 + \boldsymbol{p} \\ \omega_1 = \omega_2 + \omega \end{cases} , \tag{17b}$$

$$\begin{cases} \boldsymbol{p}_2 = \boldsymbol{p} + \boldsymbol{p}_1 \\ \omega_2 = \omega + \omega_1 \end{cases} . \tag{17c}$$

Now let us assume that the wave action is independent of the direction of the horizontal wavenumber,

$$n_{\boldsymbol{p}} = n(|\boldsymbol{k}|, |m|).$$

Note that value of the interaction matrix element is independent of horizontal azimuth as it depends only on the magnitude of interacting wavenumbers. Therefore one can integrate the kinetic equation (1) over horizontal azimuth[14], yielding

$$\frac{\partial n_{\boldsymbol{p}}}{\partial t} = \frac{2}{k} \int \left(R_{12}^0 - R_{20}^1 - R_{01}^2 \right) dk_1 dk_2 dm_1 dm_2 ,$$
$$R_{12}^0 = f_{\boldsymbol{p}_1 \boldsymbol{p}_2}^{\boldsymbol{p}} \left| V_{\boldsymbol{p}_1 \boldsymbol{p}_2}^{\boldsymbol{p}} \right|^2 \delta_{m-m_1-m_2} \delta_{\omega_{\boldsymbol{p}} - \omega_{\boldsymbol{p}_1} - \omega_{\boldsymbol{p}_2}} k k_1 k_2 / S_{1,2}^0 .$$
$$\tag{18}$$

Here $S_{1,2}^0$ appears as the result of integration of the horizontal-momentum conservative delta function over all possible orientations and is equal to the area of the triangle with sides with the length of the horizontal wavenumbers $k = |\boldsymbol{k}|$, $k_1 = |\boldsymbol{k}_1|$ and $k_2 = |\boldsymbol{k}_2|$. This is the form of the kinetic equation which will be used to find scale-invariant solutions in the next section.

III. SCALE-INVARIANT KINETIC EQUATION

A. Reduction of Kinetic Equation to the Resonant Manifold

In the high-frequency limit $\omega \gg f$, one could conceivably neglect the effects of the rotation of the Earth. The dispersion relation (12) then becomes

$$\omega_{\boldsymbol{p}} \equiv \omega_{\boldsymbol{k},m} \simeq \frac{g}{\rho_0 N} \frac{|\boldsymbol{k}|}{|m|} , \tag{19}$$

and, to the leading order, the matrix element (15) retains only its first term, $I_{\boldsymbol{p},\boldsymbol{p}_1,\boldsymbol{p}_2}$.

The azimuthally-integrated kinetic equation (18) includes integration over k_1 and k_2 since the integrations over m_1 and m_2 can be done by using delta functions. To use delta functions, we need to perform what is called reduction to the resonant manifold. Consider, for example, resonances of type (17a). Given k, k_1, k_2 and m, one can find m_1 and m_2 satisfying the resonant condition by solving simultaneous equations

$$m = m_1 + m_2, \qquad \frac{k}{|m|} = \frac{k_1}{|m_1|} + \frac{k_2}{|m - m_1|}. \tag{20}$$

The solutions of this quadratic equation are given by

$$m_1 = \frac{m}{2k} \left(k + k_1 + k_2 + \sqrt{(k + k_1 + k_2)^2 - 4kk_1} \right)$$
$$m_2 = m - m_1., \tag{21a}$$
$$\text{and}$$
$$m_1 = \frac{m}{2k} \left(k - k_1 - k_2 - \sqrt{(k - k_1 - k_2)^2 + 4kk_1} \right)$$
$$m_2 = m - m_1.. \tag{21b}$$

Note that Eq. (21a) translates into Eq. (21b) if the indices 1 and 2 are exchanged. Similarly, resonances of type (17b) yield

$$m_2 = -\frac{m}{2k}\left(k - k_1 - k_2 + \sqrt{(k - k_1 - k_2)^2 + 4kk_2}\right)$$
$$m_1 = m + m_2.,$$

(22a)

and

$$m_2 = -\frac{m}{2k}\left(k + k_1 - k_2 + \sqrt{(k + k_1 - k_2)^2 + 4kk_2}\right)$$
$$m_1 = m + m_2.$$

(22b)

and resonances of type (17c) yield

$$m_1 = -\frac{m}{2k}\left(k - k_1 - k_2 + \sqrt{(k - k_1 - k_2)^2 + 4kk_1}\right)$$
$$m_2 = m + m_1.,$$

(23a)

and

$$m_1 = -\frac{m}{2k}\left(k - k_1 + k_2 + \sqrt{(k - k_1 + k_2)^2 + 4kk_1}\right)$$
$$m_2 = m + m_1..$$

(23b)

After this reduction, a double integral over k_1 and k_2 is left. The domain of integration is further restricted by the triangle inequalities

$$k < k_1 + k_2, \quad k_1 < k + k_2, \quad \text{and} \quad k_2 < k + k_1.$$

(24)

These conditions ensure that one can construct a triangle out of the wavenumbers with lengths k, k_1 and k_2 and determine the domain in the (k_1, k_2) plane called the *kinematic box* in the oceanographic literature.

Numerical evaluation of the collision integral is a complicated yet straightforward task. Interpretation of the results, though, is more difficult, mostly due to the complexity of the interaction matrix element and the nontrivial nature of the resonant set. Starting with McComas and Bretherton[6], therefore, predictions were made based on a further simplification. This simplification is based on the assertion that it is interactions between wavenumbers with extreme scale separation that contribute mostly to the nonlinear dynamics. Three main classes of such resonant triads appear, characterized by extreme scale separation. These three main classes are

- the vertical backscattering of a high-frequency wave by a low-frequency wave of twice the vertical wavenumber into a second high-frequency wave of oppositely signed vertical wavenumber. This type of scattering, as in Eqs. (25a, 27b, 29a, 30a) below, is called elastic scattering (ES).

- The scattering of a high-frequency wave by a low-frequency, small-wavenumber wave into a second, nearly identical, high-frequency large-wavenumber wave. This type of scattering, as in Eqs. (25b, 27a, 29b, 30b) below, is called induced diffusion (ID).

- The decay of a small-wavenumber wave into two large vertical-wavenumber waves of approximately one-half the frequency. This type of scattering, as in Eqs. (26a, 26b, 28a, 28b) below, is called parametric subharmonic instability (PSI).

To see how this classification appears analytically, we perform the limit of $k_1 \to 0$ and the limit $k_1 \to \infty$ in Eqs (21–23). We will refer to the k_1 *or* $k_2 \to 0$ limits as IR limits, while the k_1 *and* $k_2 \to \infty$ limit will be referred as an UV limit. Since the integrals in the kinetic equation for power-law solutions will be dominated by the scale-separated interaction, this will help us analyze possible solutions to the kinetic equation.

The results of the $k_1 \to 0$ limit of Eqs. (21–23) are given by

$$\begin{cases} m_1 \to 2m, m_2 \to -m \\ \omega_1 \ll \omega, \omega_2 \sim \omega \end{cases},$$

(25a)

$$\begin{cases} -m_1 \ll m, m_2 \sim m \\ \omega_1 \ll \omega, \omega_2 \sim \omega \end{cases},$$

(25b)

$$\begin{cases} m_1 \ll m, m_2 \sim -m \\ \omega_1 \sim 2\omega, \omega_2 \sim \omega \end{cases}, \tag{26a}$$

$$\begin{cases} -m_1 \ll m, m_2 \sim -m \\ \omega_1 \sim 2\omega, \omega_2 \sim \omega \end{cases}, \tag{26b}$$

$$\begin{cases} -m_1 \ll m, m_2 \sim m \\ \omega_1 \ll \omega, \omega_2 \sim \omega \end{cases}, \tag{27a}$$

$$\begin{cases} m_1 \to -2m, m_2 \to -m \\ \omega_1 \ll \omega, \omega_2 \sim \omega \end{cases}. \tag{27b}$$

We now see that the interactions (25a, 27b) correspond to the elastic scattering (ES) mechanism, the interactions (25b, 27a, correspond to the induced diffusion (ID). The interactions (26a, 26b), correspond to the parametric subharmonic instability (PSI).

Similarly, taking the k_1 and $k_2 \to \infty$ limits, of Eqs. (21–23) we obtain

$$\begin{cases} m_1 \gg m, -m_2 \gg m \\ \omega_1, \omega_2 \sim \omega/2 \end{cases}, \tag{28a}$$

$$\begin{cases} -m_1 \gg m, m_2 \gg m \\ \omega_1, \omega_2 \sim \omega/2 \end{cases}, \tag{28b}$$

$$\begin{cases} m_1 \sim m/2, m_2 \sim -m/2 \\ \omega_1, \omega_2 \gg \omega \end{cases}, \tag{29a}$$

$$\begin{cases} -m_1 \gg m, -m_2 \gg m \\ \omega_1, \omega_2 \gg \omega \end{cases}, \tag{29b}$$

$$\begin{cases} m_1 \sim -m/2, m_2 \sim m/2 \\ \omega_1, \omega_2 \gg \omega \end{cases}, \tag{30a}$$

$$\begin{cases} -m_1 \gg m, -m_2 \gg m \\ \omega_1, \omega_2 \gg \omega \end{cases}. \tag{30b}$$

We now can identify the interactions (28a, 28b) to be PSI, the interactions (29a, 30a) to be ES, and finally the interactions (29b, 30b) as being ID.

This classification provides an easy and intuitive tool for describing extremely scale-separated interactions. We will see below that one of these interactions, namely ID, explain reasonably well the experimental data that is available to us.

B. Convergences and divergences of the kinetic equation.

Neglecting the effects of the rotation of the Earth yields a scale-invariant system with dispersion relation given by Eq. (19) and matrix element given only by the I_{p,p_1,p_2} in Eq. (15). This is the kinetic equation of Refs. 5,34, describing internal waves in hydrostatic balance in a non-rotating environment.

Proposing a self-similar separable spectrum of the form (2), it is clear from the bi-homogeneous nature of the azimuthally-integrated kinetic equation (18) that

$$\frac{\partial n(\alpha\boldsymbol{k}, \beta m)}{\partial t} = \alpha^{4-2a}\beta^{1-2b}\frac{\partial n(\boldsymbol{k}, m)}{\partial t}. \tag{31}$$

In order to find a steady scale-invariant solution for all values of k and m, it is therefore sufficient to find exponents that give zero collision integral for one wavenumber. One can fix k and m, adopting for instance $k = m = 1$, and seek zeros of the collision integral as a function of a and b:

$$\frac{\partial n(k = 1, m = 1)}{\partial t} \equiv \mathcal{C}(a, b). \tag{32}$$
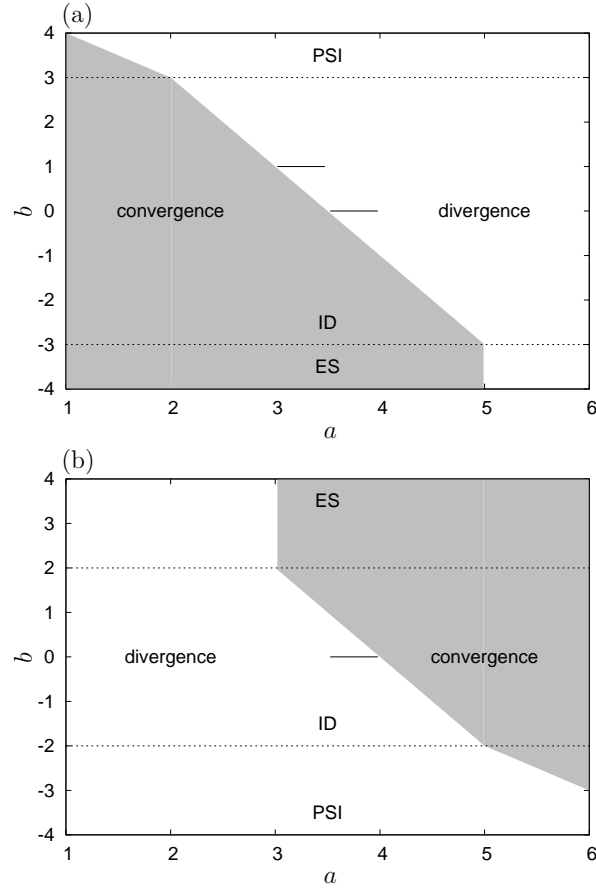
FIG. 2: Divergence/convergence due to IR wavenumbers (top) and due to UV wavenumbers (bottom). The integral converge for the exponents in the shaded regions or on the segments $(b = 0, 7/2 < a < 4)$ and $(b = 1, 3 < a < 7/2)$. Dashed lines distinguish the domains where the indicated named triads dominate the singularity.

Before embarking on numerical or analytical integration of the kinetic equation (18) with scale-invariant solutions (2), it is necessary to check whether or not the collision integral converges. Appendix A outlines these calculations. The condition for the scale-invariant collision integral (32) to converge at the IR end, k_1 or $k_2 \rightarrow 0$ is given by

$$a + b/2 - 7/2 < 0 \quad \text{and} \quad -3 < b < 3, \tag{33a}$$

$$a - 4 < 0 \quad \text{and} \quad b = 0, \tag{33b}$$

$$a - 7/2 < 0 \quad \text{and} \quad b = 1, \tag{33c}$$

$$a + b - 5 < 0 \quad \text{and} \quad b > 3, \tag{33d}$$

or

$$a - 5 < 0 \quad \text{and} \quad b < -3. \tag{33e}$$

Similarly, UV convergence as k_1 and $k_2 \rightarrow \infty$ implies that

$$a + b/2 - 4 > 0 \quad \text{and} \quad -2 < b < 2, \tag{34a}$$

$$a - 7/2 > 0 \quad \text{and} \quad b = 0, \tag{34b}$$

$$a - 3 > 0 \quad \text{and} \quad b > 2, \tag{34c}$$

or

$$a + b - 3 > 0 \quad \text{and} \quad b < -2. \tag{34d}$$

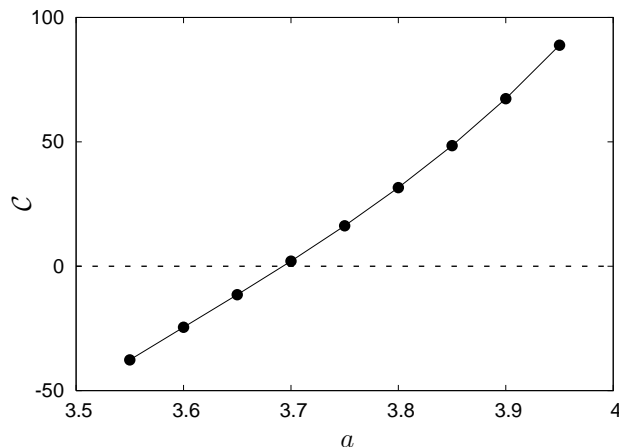The domains of divergence and convergence are shown in Fig. 2.

FIG. 3: Value of the collision integral as a function of a on the convergent segment, $b = 0$.

Figure 2 also displays the classes of triads dominating the interactions. Knowing the classes of interactions that lead to the divergences of the kinetic equation allows us to find possible physical scenarios of the convergent solutions or to find a possible physical regularization of the divergences.

Note that in addition to the two-dimensional domain of IR convergence [the regions (33a, 33d, 33e)] there are two additional IR convergent line segments given by Eqs. (33b) and (33c). These two special line segments appear because of the $b(b-1)$ prefactor to the divergent contributions to the collision integral (A3). Similarly, for the UV limit, in addition to the two-dimensional region of convergence (34a, 34c, 34d) there is an additional special line segment of $b = 0$ (34b).

We see that these domains of convergence overlap only on the segment

$$7/2 < a < 4 \ \text{ and } \ b = 0\,. \tag{35}$$

Note that $b = 0$ corresponds to wave action independent of vertical wavenumbers, $\partial n/\partial m = 0$. Existence of the $b = 0$ line will allow us to find novel convergent solution in Sec. IV. We also note that the IR segment on $b = 0$ coincides with one of the ID solution determined in Sec. VI. The other segment on $b = 1$ do not coincides with the ID solution in Sec. VI since the scale-invariant system has higher symmetry than the system with Coriolis effect.

IV. A NOVEL CONVERGENT SOLUTION

To find out whether there is a steady solution of the kinetic equation along the convergent segment (35), we substitute the power-law ansatz (2) with $b = 0$ into the azimuthally-integrated kinetic equation (18). We then compute numerically the collision integral as a function of a for $b = 0$. To this end, we fix $k = m = 1$ and perform a numerical integration over the kinematic box (24), reducing the integral to the resonant manifold as described in Sec. III A.

The result of this numerical integration is shown in Fig. 3. The figure clearly shows the existence of a steady solution of the kinetic equation (18) near $a \cong 3.7$ and $b = 0$.

This is, therefore, *the only convergent steady solution* to the scale-invariant kinetic equation for the internal wave field. It is highly suggestive that it should exist so close to the GM spectrum, $a = 4$ and $b = 0$ for large wavenumbers, the most agreed-upon fit to the spectra observed throughout the ocean. It remains to be seen whether how this solution is modified by inclusion of background rotation.

V. BALANCE BETWEEN DIVERGENCES

The fact that the collision integral $\mathcal{C}$ diverges for almost all values of a and b can be viewed both as a challenge and as a blessing. On the one hand, it makes the prediction of steady spectral slopes more difficult, since it now depends on the details of the truncation of the domain of the integration. Fortunately, it provides a powerful tool for quantifying the effects of fundamental players in ocean dynamics, most of which live on the fringes of the inertial
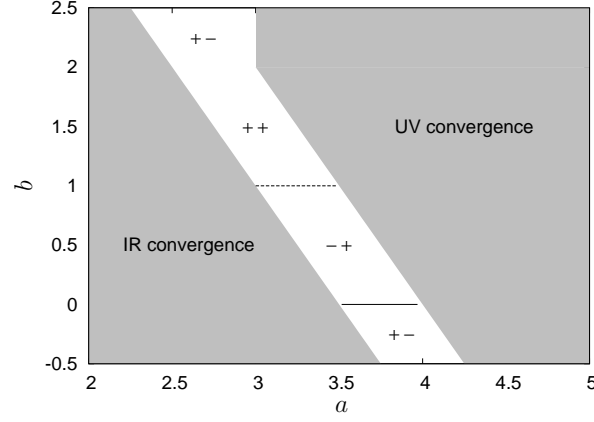
FIG. 4: Signs of the divergences where the both IR and UV contributions diverge. The left symbols show the signs due to IR wavenumbers and the right symbols show the signs due to UV wavenumbers.

subrange of the internal wave field: the Coriolis effect, as well as tides and storms at the IR end of the spectrum, and wave breaking and dissipation at the UV end. The sensitive response of the inertial subrange to the detailed modeling of these scale-separated mechanisms permits, in principle, building simple models in which these are the only players, bypassing the need to consider the long range of wave scales in between.

At the IR end, the resonant interactions are dominated by the ID singularity for $-3 < b < 3$, Fig. 2. The sign of the divergences is given by $-b(b-1)$ (Eq. (A3)). Similarly, at the UV end resonant interactions are dominated by the ID singularity for $-2 < b < 2$ (Fig. 2). The sign of the divergence is given by b (Eq. (A4)). At the UV end for $b > 2$, where ES determines the divergences, the sign of the singularity is given by $-b$, i.e. the sign is negative (Eq. (A5)). Figure 4 shows the signs of the divergences where both the IR and UV contributions diverge: the left sign corresponds to the IR contribution, and the right sign to the UV contribution.

Hence, in the regions,

$$7 < 2a + b < 8, \text{ and } -2 < b < 1, \tag{36a}$$

or

$$7 < 2a + b, a < 3, \text{ and } b > 2, \tag{36b}$$

the divergences of the collision integral at the IR and UV ends have opposite signs. Then formal solutions can be constructed by having these two divergences cancel each other out.

This observation justifies the existence of the PR solution (5). Indeed, the PR spectrum has divergent power-law exponents at the both ends. One can prove that the PR spectrum is an exact steady solution of the kinetic equation (1) by applying the Zakharov–Kuznetsov conformal mapping for systems with cylindrical symmetry[35,36,37]. This Zakharov–Kolmogorov conformal mapping effectively establishes a map between the neighborhoods of zero and infinity. Making these two contributions cancel point-wisely yields the solution (5). For this transformation to be mathematically applicable the integrals have to converge. This transformation leads only to a formal solution for divergent integrals.

The PR spectrum was first found by Pelinovsky and Raevsky[11]. However, they realized that it was only a formal solution. The solution was found again in Ref. 1 through a renormalization argument, and in Ref. 5 within an isopycnal formulation of the wave field.

The idea of a formal solution, such as PR, can be generalized quite widely: in fact, *any* point in the regions with opposite-signed divergences can be made into a steady solution under a suitable mapping that makes the divergences at zero and infinity cancel each other, as does the Kuznetsov–Zakharov transformation. Such *generalized* Kuznetsov–Zakharov transformation is an extension of the idea of principle value for a divergent integral, whereby two divergent contributions are made to cancel each other through a specific relation between their respective contributions.

This scenario also suggests an possible explanation for the variability of the power-law exponents of the quasi-steady spectra: inertial subrange spectral variability is to be expected when it is driven by the nonlocal interactions. The natural local variability of players outside the inertial range, such as tides and storms, translates into a certain degree of non-universality.

VI.   REGULARIZATION BY THE CORIOLIS EFFECT

Physically, ocean does not perform generalized Kuznetsov–Zakharov transformation. However, in the ocean there are finite boundaries in frequency domain. In particular, the inertial frequency, f, provides a truncation for the IR part of the spectrum, while the UV truncation is provided by the buoyancy frequency, N. These two frequencies vary from place to place, giving grounds for spectral variability. Consequently, the integrals are not truly divergent, rather they have a large numerical value dictated by the location of the IR cutoff.

All the experimental points are located in regions of the (a, b) domain $a > (-b+7)/2$ for which the integral diverges in the IR region. For most of the experimental points, the UV divergence is not an issue, as $a > -b/2 + 4$. The UV region is therefore assumed to be either sub-dominant or convergent in this section, where we study the regularization resulting from a finite value of f.

Since the IR cutoff is given by f, a frequency, it is easier to analyze the resulting integral in (ω_1, m_1) rather than in the traditional (k_1, m_1) domain. Thus we need to express both the kinetic equation and the kinematic box in terms of frequency and vertical wavenumber. For this, we use the dispersion relation (12) to express k in terms of ω in the description of the kinematic box (24):

$$
\begin{aligned}
&\omega_1 < E_3(m_1),\ \omega_1 > E_4(m_1),\ \omega_1 > E_1(m_1) \\
&\quad \text{if } m_1 < 0,\ \omega_1 > \omega, \\
&\omega_1 > E_3(m_1),\ \omega_1 < E_4(m_1),\ \omega_1 < E_1(m_1) \\
&\quad \text{if } m_1 < 0,\ \omega_1 < \omega, \\
&\omega_1 < E_2(m_1),\ \omega_1 > E_2(m_1),\ \omega_1 > E_4(m_1) \\
&\quad \text{if } m_1 > 0,\ \omega_1 < \omega, \\
&\omega_1 > E_3(m_1),\ \omega_1 < E_1(m_1),\ \omega_1 < E_2(m_1) \\
&\quad \text{if } m_1 > 0,\ \omega_1 > \omega,
\end{aligned}
$$

(37a)
(37b)
(37c)
(37d)

where we have introduced the four curves in the (ω_1, m_1) domain that parameterize the kinematic box:

$$
\begin{aligned}
E_1(\omega_1) &= m \frac{-\sqrt{-f^2 + \omega^2} + \sqrt{-f^2 + (\omega - \omega_1)^2}}{\sqrt{-f^2 + \omega_1^2} + \sqrt{-f^2 + (\omega - \omega_1)^2}}, \\
E_2(\omega_1) &= m \frac{\sqrt{-f^2 + \omega^2} + \sqrt{-f^2 + (\omega - \omega_1)^2}}{\sqrt{-f^2 + \omega_1^2} + \sqrt{-f^2 + (\omega - \omega_1)^2}}, \\
E_3(\omega_1) &= m \frac{-\sqrt{-f^2 + \omega^2} + \sqrt{-f^2 + (\omega - \omega_1)^2}}{-\sqrt{-f^2 + \omega_1^2} + \sqrt{-f^2 + (\omega - \omega_1)^2}}, \\
E_4(\omega_1) &= m \frac{\sqrt{-f^2 + \omega^2} + \sqrt{-f^2 + (\omega - \omega_1)^2}}{-\sqrt{-f^2 + \omega_1^2} + \sqrt{-f^2 + (\omega - \omega_1)^2}}.
\end{aligned}
$$

The *kinematic box* in the (ω, m) domain is shown in Fig. 5. To help in the transition from the traditional kinematic box to the kinematic box in (ω, m) domain, the following limits were identified:

- ID1 is the ID limit of Eq. (25b) with indices 1 and 2 being flipped

- ID2 is the ID limit of Eq. (27a) with indices 1 and 2 being flipped

- ID3 is the ID limit of Eq. (25b)

- ID4 is the ID limit of Eqs. (29b, 30b)

- PSI1 is the PSI limit of Eq. (28a)

- PSI2 is the PSI limit of Eq. (28b)

- PSI3 is the PSI limit of Eq. (26a)

- PSI4 is the PSI limit of Eq. (26b)

- ES1 is the ES limit of Eq. (25a)

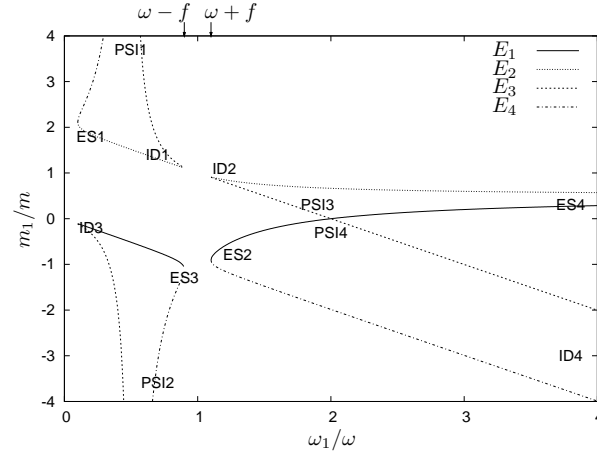- ES2 is the ES limit of Eq. (27b) with indices 1 and 2 being flipped

FIG. 5: The kinematic box in the (ω_1, m_1) domain. Two disconnected regions where $\omega_1 < \omega$ depict regions with "sum" interactions, namely $\omega = \omega_1 + \omega_2$, $m = m_1 + m_2$, type of the resonances. The connected regions where $\omega_1 > \omega$ depict "difference" resonances, $\omega_2 = \omega_1 - \omega$, $m_2 = m_1 - m$. The parameters are chosen so that $f/\omega = 0.1$.

- ES3 is the ES limit of Eq. (27b) with indices 1 and 2 being flipped

- ES4 is the ES limit of Eq. (29a)

An advantage of the (ω, m) presentation for the kinematic box is that it allows a transparent reduction to the resonant manifold. A disadvantage is the curvilinear boundaries of the box, requiring more sophisticated analytical treatment. To proceed, we assume a power-law spectrum, similar to Eq. (2), but in the (ω, m) space:

$$n_{\omega,m} \propto \omega^{\widetilde{a}} m^{\widetilde{b}}. \tag{38}$$

We need to transform the wave action as a function of k and m to a function of ω and m. This is done in Appendix B. The relation between a, b and $\widetilde{a}$, $\widetilde{b}$ reads:

$$\widetilde{a} = -a, \quad \widetilde{b} = -a - b.$$

Equation (18) transforms into

$$
\begin{aligned}
\frac{\partial}{\partial t} n(k(\omega, m), m) \; = \; & \frac{1}{k} \int d\omega_1 dm_1 J \frac{|V_{12}^0|^2}{S_{1,2}^0} \left(n_1 n_2 - n(n_1 + n_2) \right)\Big|_{\omega_2 = \omega - \omega_1, m_2 = m - m_1} \\
& - \frac{2}{k} \int d\omega_1 dm_1 J \frac{|V_{02}^1|^2}{S_{2,0}^1} \left(n n_2 - n_1(n + n_2) \right)\Big|_{\omega_2 = \omega_1 - \omega, m_2 = m_1 - m}
\end{aligned}
\tag{39}
$$

We have used the dispersion relation $k_i = m_i \sqrt{\omega_i^2 - f^2}$, and defined J as the Jacobian of the transformation from (k_1, k_2) into (ω_1, ω_2), times the $k k_1 k_2$ factor,

$$J = k k_1 k_2 \frac{dk_1}{d\omega_1} \frac{dk_2}{d\omega_2}.$$

In Fig. 5, there are three ID corners with significant contribution to the collision integral:

1. ID1 region. In this region, m_1 is slightly bigger than m, ω_1 slightly smaller than ω, and ω_2 and m_2 are both very small. This region can be obtained from the region (37b) above by interchanging indices 1 and 2. In this region,

$$n_2 \gg n, \, n_1.$$

2. ID2 region. In this region, ω_1 is slightly bigger than $\omega + f$ where $\omega_2 = \omega_1 - \omega$ is small, and $m_2 = m_1 - m$ is negative and small. This is the region (37d). Also

$$n_2 \gg n, \, n_1.$$

3. ID3 region. Small ω_1, small negative m_1. This corresponds to the region (37b), where

$$n_1 \gg n, \, n_2.$$

Note that this region can be obtained from the region ID1 by flipping indices 1 and 2. Consequently, only one of the ID1, ID2 should be taken into account, with a factor of two multiplying the respective contribution.

Making these simplification, and taking into account the areas of integration in the kinematic box, we obtain

$$\frac{\partial}{\partial t} n(k(\omega, m), m) = \frac{2}{k} \int_{f}^{f+\omega_s} d\omega_1 \int_{E_3(\omega_1)}^{E_1(\omega_1)} dm_1 J \frac{|V_{1,2}^0|^2}{S_{1,2}^0} n_1(n_2 - n) - \frac{2}{k} \int_{\omega-f-\omega_s}^{\omega-f} d\omega_1 \int_{E_3(\omega_1)}^{E_1(\omega_1)} dm_1 J \frac{|V_{1,0}^2|^2}{S_{1,0}^2} n_2(n - n_1),$$
(40)

where the small parameter ω_s is introduced to restrict the integration to a neighborhood of the ID corners. The arbitrariness of the small parameter will not affect the end result below.

To quantify the contribution of near-inertial waves to a (ω, m) mode, we write

$$\epsilon \sim f \ll \omega = 1.$$

Subsequently, near the region ID3 of the kinematic box, we write

$$\omega_1 = f + \epsilon,$$

while near the ID2 corners of the kinematic box we write

$$\omega_1 = \omega + f + \epsilon.$$

We then expand the resulting analytical expression (40) in powers of ϵ and f without making any assumptions on their relative size. These calculations, including the integration over vertical wavenumbers m_1, are presented in Appendix C. The resulting expression for the kinetic equation is given by

$$\frac{\partial}{\partial t} n(k(\omega, m), m) = \frac{\pi}{4k} \left(\widetilde{a} - \widetilde{b} \right) \left(\widetilde{a} - 3 \left(3 + \widetilde{b} \right) \right)$$
$$\times m^{5+2\widetilde{b}} \omega^{-3+\widetilde{a}-\widetilde{b}} \int_0^\mu d\epsilon (\epsilon + f)^{4+\widetilde{a}+\widetilde{b}} (\epsilon^2 + 2\epsilon f + 17 f^2) \,.$$
(41)

The integral over ϵ diverges at $\epsilon = 0$, if $f = 0$ and if $6 + \widetilde{a} + \widetilde{b} > -1$.[39]

However, if we postpone taking $f = 0$ limit, we see that the integral is zero to leading order if

$$\widetilde{a} - 3 \left(3 + \widetilde{b} \right) = 0 \quad \text{or} \quad \widetilde{a} - \widetilde{b} = 0$$
(42)

or, in terms of a and b,

$$9 - 2a - 3b = 0 \quad \text{or} \quad b = 0.$$
(43)

This is the family of power-law steady-state solutions to the kinetic equations dominated by infra-red ID interactions. These steady states are identical to the ID stationary states identified by McComas and Bretherton[6], who derived a diffusive approximation to their collision integral in the infra-red ID limit. Note that McComas and Müller[16] interpreted $b = 0$ as a no action flux in vertical wavenumber domain, while $9 - 2a - 3b = 0$ is a constant action flux solution. What is presented in this section is a rigorous asymptotic derivation of this result. These ID solutions helps us to interpret observational data of Fig. 1 that is currently available to us.

VII. CONCLUSIONS

The results in this paper provide an interpretation of the variability in the observed spectral power laws. Combining Figs. 1, 2 and 4 with Eqs. (4), (5) and (43), produces the results shown in Fig 6.
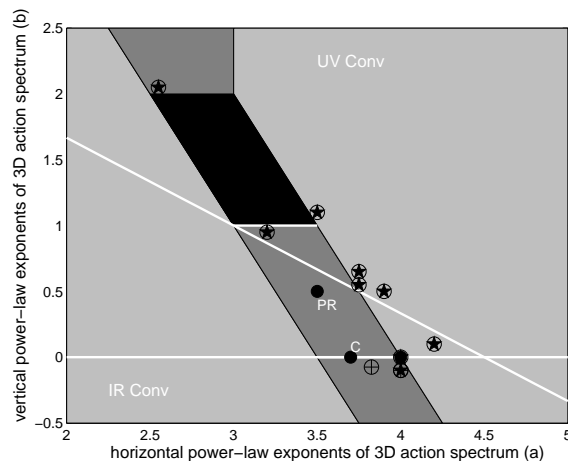
FIG. 6: The observational points and the theories. The filled circles represent the Pelinovsky–Raevsky (PR) spectrum, the convergent numerical solution determined in Section 4 and the GM spectrum. Circles with stars represent power-law estimates based upon one-dimensional spectra. Circles with cross hairs represent estimates based upon two-dimensional data sets. See Fig. 1 for the identification of the field programs. Light grey shading represents regions of the power-law domain for which the collision integral converges in either the IR or UV limit. The dark grey shading represents the region of the power-law domain for which neither the IR or UV limits converge. The region of black shading represents the sub-domain for which the IR and UV divergences have the same sign. Overlain as solid white lines are the induced diffusion stationary states.

Notice that most of the observational points are UV convergent and IR divergent and that regularization of the collision integral by f, as in Sec. VI, produces a family of stationary states that collapses much of the variability. Four points land in the region where the spectra are both IR and UV divergent, with all but one point close to the ID lines. None of the observations lies in a region where both IR and UV divergences have the same sign. Furthermore, the novel convergent (non-rotating) solution is in close proximity to the experimental points determined from the two-dimensional spectra.

Summarizing the paper, we have analyzed the scale-invariant kinetic equation for internal gravity waves, and shown that its collision integral diverges for almost all spectral exponents. Figure 6 shows that the integral nearly always diverges, either at zero or at infinity. This means that, in the wave turbulence kinetic equation framework, the energy transfer is dominated by the scale-separated interactions with either large or small scales.

The only exception where the integral converges is a segment of a line, $7/2 < a < 4$, with $b = 0$. On this convergent segment, we found a special solution, $(a, b) = (3.7, 0)$. This new solution is not far from the large-wavenumber asymptotic form of the Garrett–Munk spectrum, $(a, b) = (4, 0)$.

We have argued that there exist two regions of power-law exponents which can yield quasi-steady solutions of the kinetic equation. For these ranges of exponents, the contribution of the scale-separated interactions due to the IR and UV wavenumbers can be made to balance each other. The Pelinovsky–Raevsky spectrum is a special case of this scenario. None of the observational power-law exponents lie within the region of same-signed UV and IR divergences.

This scenario, in which the energy spectrum in the inertial subrange is determined by the nonlocal interactions, provides an explanation for the variability of the power-law exponents of the observed spectra: they are a reflection of the variability of dominant players outside of the inertial range, such as the Coriolis effect, tides and storms. can not be universal.

We also rederive ID steady-solution lines, which are also shown as white lines in Fig. 6.

All of theory, experimental data, and the results of numerical simulation in Ref. 38 hint at the importance of the IR contribution to the collision integral. The nonlocal interactions with large scales will therefore play a dominant role in forming the internal-wave spectrum. To the degree that the large scales are location dependent and not universal, the high-frequency, high vertical-wavenumber internal-wave spectrum ought to be affected by this variability. Consequently, the internal-wave spectrum should be strongly dependent on the regional characteristics of the ocean.

TABLE I: Asymptotics as $k_1 \to 0$. ES (21a, 23b) gives ϵ^{-a+5} owing to the symmetry of y. ID (21b, 23a) gives $\epsilon^{-a-(b-7)/2}$ (ϵ^{-a+4}) owing to the second cancellation. PSI (22a, 22b) gives ϵ^{-a-b+5}. The asymptotics for $b = 0$ appear in parentheses.

	m_1	m_2	ω_1	ω_2	$V_{\boldsymbol{p}_j\boldsymbol{p}_k}^{\boldsymbol{p}_i}$	$f_{\boldsymbol{p}_j\boldsymbol{p}_k}^{\boldsymbol{p}_i}$	$g_{j,k}^{i\prime}$	$T_{j,k}^i$
(21a)	ϵ^0	ϵ^0	ϵ^1	ϵ^0	$\epsilon^{1/2}$	ϵ^{-a+1}	ϵ^0	ϵ^{-a+2}
(21b)	$\epsilon^{1/2}$	ϵ^0	$\epsilon^{1/2}$	ϵ^0	$\epsilon^{1/4}$	$\epsilon^{-a-(b-1)/2}$ $\left(\epsilon^{-a+1}\right)$	ϵ^0	$\epsilon^{-a-b/2+1}$ $\left(\epsilon^{-a+3/2}\right)$
(22a)	ϵ^1	ϵ^0	ϵ^0	ϵ^0	ϵ^1	ϵ^{-a-b}	ϵ^{-1}	ϵ^{-a-b+3}
(22b)	ϵ^1	ϵ^0	ϵ^0	ϵ^0	ϵ^1	ϵ^{-a-b}	ϵ^{-1}	ϵ^{-a-b+3}
(23a)	$\epsilon^{1/2}$	ϵ^0	$\epsilon^{1/2}$	ϵ^0	$\epsilon^{1/4}$	$\epsilon^{-a-(b-1)/2}$ $\left(\epsilon^{-a+1}\right)$	ϵ^0	$\epsilon^{-a-b/2+1}$ $\left(\epsilon^{-a+3/2}\right)$
(23b)	ϵ^0	ϵ^0	ϵ^1	ϵ^0	$\epsilon^{1/2}$	ϵ^{-a+1}	ϵ^0	ϵ^{-a+2}

APPENDIX A: ASYMPTOTICS OF COLLISION INTEGRAL IN INFRA-RED AND ULTRA-VIOLET LIMITS

Let us integrate Eq. (18) over m_1 and m_2.

$$
\begin{aligned}
\frac{\partial n_{\boldsymbol{p}}}{\partial t} &= \frac{1}{k} \int \left(T_{1,2}^0 - T_{2,0}^1 - T_{0,1}^2\right) dk_1 dk_2, \\
T_{1,2}^0 &= k k_1 k_2 |V_{\boldsymbol{p}_1\boldsymbol{p}_2}^{\boldsymbol{p}}|^2 f_{\boldsymbol{p}_1\boldsymbol{p}_2}^{\boldsymbol{p}} / (|g_{1,2}^{0\prime}|S_{1,2}^0), \\
g_{1,2}^{0\prime}(k_1,k_2) &= \left.\frac{dg_{1,2}^0(m_1)}{dm_1}\right|_{m_1=m_1^*(k_1,k_2)}, \\
g_{1,2}^0(m_1) &= \frac{k}{m} - \frac{k_1}{|m_1|} - \frac{k_2}{|m-m_1|},
\end{aligned}
\tag{A1}
$$

where $g_{1,2}^{0\prime}$ appears owing to $\delta_{\omega_{\boldsymbol{p}}-\omega_{\boldsymbol{p}_1}-\omega_{\boldsymbol{p}_2}}$ and $m_1^*(k_1,k_2)$ is given by the resonant conditions (21)–(23).

1. Infra-red asymptotics

We consider the asymptotics of the integral in Eq. (A1) as $k_1 \to 0$. We employ the independent variables x and y, where $k_1 = kx$, $k_2 = k(1+y)$, $x, y = O(\epsilon)$, $x > 0$ and $-x < y < x$. In this limit of $\epsilon \to 0$, $n_1 \gg n, n_2$. In this limit, Eqs. (21a) and (23b), Eqs. (21b) and (23a), and Eqs. (22a) and (22b) correspond to ES, Eqs. (25a, 27b) ID, Eqs. (25b, 27a), PSI, Eqs. (25a, 27b), respectively. Without loss of generality m is set to be positive.

Assuming the power-law spectrum, $n(\boldsymbol{k}, m) = |\boldsymbol{k}|^{-a}|m|^{-b}$, we make Taylor expansion for the integrand of the kinetic equation (A1) as powers of ϵ, that is x and y. Then, we get Table I which shows the leading orders of the each terms according to the asymptotics. The leading order of the collision integral is given by ID when $-3 < b < 3$. Therefore, we are going to show the procedure to get the leading order of ID (21b) and (23a) below.

As $\epsilon \to 0$, $n_2 \to n$ for ID solutions. Therefore, the leading orders of $f_{1,2}^0 \sim n_1(n_2 - n)$ and $f_{0,1}^2 \sim n_1(n - n_2)$ is $O(\epsilon^{-a-(b-1)/2})$. The order $O(\epsilon^{-a-b/2})$ is canceled as $\epsilon \to 0$. This is called the *first cancellation*. It must be noted that the leading order when $b = 0$ is $1/2$ larger than that when $b \neq 0$ since $\partial n/\partial m = 0$. The leading orders when $b = 0$ are written in parentheses in Table I.

The leading order of the integrand in Eq. (A1) is written as

$$
\begin{aligned}
T_{1,2}^0 - T_{2,0}^1 - T_{0,1}^2 &\propto k^{-2a+3}m^{-2b+1}\frac{x^{-a-(b+1)/2}y}{\sqrt{(x+y)(x-y)}} \\
&\times \left(-2ay^2 - b\left((1-b)y(x+y) - 2x(x-y)\right) + b(b+1)xy\right).
\end{aligned}
\tag{A2}
$$

TABLE III: Asymptotics as $k_1 \to \infty$. PSI (21a, 21b) gives ϵ^{a+b-3}. ES (22a, 23a) gives ϵ^{a-3}. ID (22b, 23b) gives $\epsilon^{a+b/2-4}$ ($\epsilon^{a-7/2}$). The asymptotics for $b = 0$ appear in parentheses.

	m_1	m_2	ω_1	ω_2	$V^{p_i}_{p_j p_k}$	$f^{p_i}_{p_j p_k}$	$g^{i\prime}_{j,k}$	$T^i_{j,k}$
(21a)	ϵ^{-1}	ϵ^{-1}	ϵ^0	ϵ^0	ϵ^0	ϵ^{a+b}	ϵ^1	ϵ^{a+b-2}
(21b)	ϵ^{-1}	ϵ^{-1}	ϵ^0	ϵ^0	ϵ^0	ϵ^{a+b}	ϵ^1	ϵ^{a+b-2}
(22a)	ϵ^0	ϵ^0	ϵ^{-1}	ϵ^{-1}	ϵ^{-1}	ϵ^a	ϵ^{-1}	ϵ^{a-2}
(22b)	$\epsilon^{-1/2}$	$\epsilon^{-1/2}$	$\epsilon^{-1/2}$	$\epsilon^{-1/2}$	ϵ^{-1}	$\epsilon^{a+b/2+1}$ $(\epsilon^{a+3/2})$	$\epsilon^{1/2}$	$\epsilon^{a+b/2-3}$ $(\epsilon^{a-5/2})$
(23a)	ϵ^0	ϵ^0	ϵ^{-1}	ϵ^{-1}	ϵ^{-1}	ϵ^a	ϵ^{-1}	ϵ^{a-2}
(23b)	$\epsilon^{-1/2}$	$\epsilon^{-1/2}$	$\epsilon^{-1/2}$	$\epsilon^{-1/2}$	ϵ^{-1}	$\epsilon^{a+b/2+1}$ $(\epsilon^{a+3/2})$	$\epsilon^{1/2}$	$\epsilon^{a+b/2-3}$ $(\epsilon^{a-5/2})$

Therefore, the integrand has $O(\epsilon^{-a-(b-5)/2})$. The term which has $O(\epsilon^{-a-b/2+2})$ is canceled since $T^2_{0,1} \to T^0_{1,2}$ (and $T^1_{2,0} \to 0$) as $\epsilon \to 0$. This is the *second cancellation*.

Finally, we get the leading order of the kinetic equation after integration over y from $-x$ to x:

$$\frac{\partial n_p}{\partial t} \propto -b(1-b)k^{4-2a}m^{1-2b}\int_0^x x^{-a-(b-5)/2}dx. \tag{A3}$$

The integral has $O(\epsilon^{-a-(b-7)/2})$. Consequently integral converges if

$$a + (b-7)/2 < 0 \quad \text{and} \quad -3 < b < 3.$$

The integral for the PR spectrum, which gives $O(\epsilon^{-1/4})$, diverges as $k_1 \to 0$. However, the integral for the GM spectrum converges because $b = 0$ and the next order is $O(1)$.

It should be noted that the leading order when $b = 1$ is $1/2$ larger than that when $b \neq 0, 1$ since a balance between first- and second-order derivative is made. The leading orders when $b = 1$ are $O(\epsilon^{-a+7/2})$. It is also helpful to note that $T^0_{1,2} - T^1_{2,0} - T^2_{1,0} = O(\epsilon^{-a+2})$ for ES because of no second cancellation. However, the collision integral has $O(\epsilon^{-a+5})$ because of symmetry of y. Therefore, the integral which is dominated by ES converges

$$a - 5 < 0 \quad \text{and} \quad b < -3.$$

Similarly, the integral which is dominated by PSI converges

$$a + b - 5 < 0 \quad \text{and} \quad b > 3.$$

2. Ultra-violet asymptotics

Next, we consider the limit $k_1 \to \infty$. In this case, k_2 also approaches to infinity. We employ the independent variables x and y as $k_1 = k/2(1+1/x+y)$ and $k_2 = k/2(1+1/x-y)$, where $x = O(\epsilon)$ and $-1 < y < 1$. Again, $m > 0$ is assumed.

The leading orders are obtained by the similar manner used in the IR asymptotic and are summarized in Table III. The leading order of the integral is given by ID, whose wavenumbers are given by Eqs. (22b, 23b), when $-2 < b < 2$. In this limit, no second cancellation is made.

As the result of the perturbation theory, we get the leading order,

$$\frac{\partial n_p}{\partial t} \propto k^{4-2a}m^{1-2b}b\int_0^x x^{a+b/2-5}dx. \tag{A4}$$

It has $O(\epsilon^{a+b/2-4})$. Therefore, the integral converges if

$$a + b/2 - 4 > 0 \quad \text{and} \quad -2 < b < 2.$$

The integral for the PR spectrum, which gives $O(\epsilon^{-1/4})$, diverges as $k_1 \to \infty$. and that for the Garrett–Munk spectrum, which gives $O(\epsilon^0)$, converges owing that $b = 0$.

Similarly,

$$\frac{\partial n_{\boldsymbol{p}}}{\partial t} \propto -k^{4-2a}m^{1-2b}b\int_0^{\infty}x^{a-2}dx \tag{A5}$$

for ES, which is dominant for $b > 2$. Consequently, the integral converges also if

$$a - 3 > 0 \ \text{and} \ b > 2.$$

In the same manner, the convergent domain of the integral for PSI is given by

$$a + b - 3 > 0 \ \text{and} \ b < -2.$$

APPENDIX B: FREQUENCY–VERTICAL-WAVENUMBER AND HORIZONTAL–VERTICAL-WAVENUMBER SPECTRUM

The theoretical work presented below addresses the asymptotic power laws of a three-dimensional action spectrum. In order to connect with that work, note that a horizontally isotropic power-law form of the three-dimensional wave action $n(\boldsymbol{k}, m)$ is given by Eq. (2).

The corresponding vertical wavenumber-frequency spectrum of energy is obtained by transforming $n_{\boldsymbol{k},m}$ from wavenumber space $(\boldsymbol{k}, m)$ to the vertical wavenumber-frequency space (ω, m) and multiplying by frequency. In the high-frequency large-wavenumber limit,

$$E(m, \omega) \propto \omega^{2-a}m^{2-a-b} \ .$$

The total energy density of the wave field is then

$$E = \int \omega(\boldsymbol{k}, m)n(\boldsymbol{k}, m) \ d\boldsymbol{k}dm = \int E(\omega, m) \ d\omega dm.$$

Thus, we also it convenient to work with the wave action spectrum expressed as a function of ω and m Therefore we also introduced (38). The relation between a, b and $\widetilde{a}$, $\widetilde{b}$ reads:

$$\widetilde{a} = -a, \quad \widetilde{b} = -a - b.$$

APPENDIX C: ASYMPTOTIC EXPANSION FOR SMALL f VALUES.

In this section we perform the small f calculations of Sec. VI. We start from the kinetic equation written as Eq. (40). There we change variables in the first line of Eq. (40) as

$$m_1 = E_3(\omega_1) + \mu(E_1(\omega_1) - E_3(\omega_1)),$$

and in the second line of Eq. (40) as

$$m_1 = E_3(\omega_1) + \mu(E_2(\omega_1) - E_3(\omega_1)).$$

Then the Eq. (40) becomes the following form:

$$\frac{\partial}{\partial t}n(k(\omega, m), m) = \frac{2}{k}\int_f^{f+\omega_{\mathrm{s}}} d\omega_1 \int_0^1 d\mu \mathcal{P}_1$$
$$- \frac{2}{k}\int_{\omega-f-\omega_{\mathrm{s}}}^{\omega-f} d\omega_1 \int_0^1 d\mu \mathcal{P}_2. \tag{C1}$$

Here we introduced integrand $\mathcal{P}_1$ and $\mathcal{P}_2$ to be

$$\mathcal{P}_1 = J\frac{|V_{1,2}^0|^2}{S_{1,2}^0}n_1(n_2 - n)(E_1(\omega_1) - E_3(\omega_1)),$$

$$\mathcal{P}_2 = J\frac{|V_{1,2}^0|^2}{S_{1,2}^0}n_2(n - n_1)(E_2(\omega_1) - E_3(\omega_1)). \tag{C2}$$

Before proceeding, note the following symmetry:

$$E_1(\omega_1 = \omega - \omega_1') = m - E_2(\omega_1'),$$

and

$$E_3(\omega_1 = \omega - \omega_1') = m - E_3(\omega_1').$$

To quantify the contribution of near-inertial waves to a (ω, m) mode, we write

$$\epsilon \sim f \ll \omega = 1.$$

Subsequently, in the domain (a) we write

$$\omega_1 = f + \epsilon,$$

in $\mathcal{P}_1$, and

$$\omega_1 = \omega + f + \epsilon$$

in $\mathcal{P}_2$. Furthermore, we expand $\mathcal{P}_1$ and $\mathcal{P}_2$ in powers of ϵ and f without making any assumptions of the relative smallness of f and ϵ. We use the facts that

$$m > 0, \quad \epsilon > 0, \quad f > 0, \quad 0 < \mu < 1.$$

Define

$$\mathcal{P}_1 = P_1 + P_2,$$

and

$$\mathcal{P}_2 = P_3 + P_4.$$

This allows us to expand P_1, P_2, P_3 and P_4 in powers of f and ϵ. We perform these calculations on Mathematica using *Series* command, and extensively using *Assumptions* field in the *FullSimplify* command.

Mathematica was then able to perform the integrals of $\mathcal{P}_1$ and $\mathcal{P}_2$ over μ from 0 to 1 in (C1) analytically. The result is given by Eq. (41).

---

[*] Author to whom should be addressed; Electronic address: nyokoyam@mail.doshisha.ac.jp

[1] P. Caillol and V. Zeitlin, "Kinetic equations and stationary energy spectra of weakly nonlinear internal gravity waves," Dyn. Atmos. Oceans **32**, 81 (2000).

[2] K. Hasselmann, "Feynman diagrams and interaction rules of wave-wave scattering processes," Rev. Geophys. **4**, 1 (1966).

[3] K. E. Kenyon, *Wave-wave scattering for gravity waves and rossby waves*, PhD thesis, UCSD, 1966.

[4] K. E. Kenyon, "Wave-wave interactions of surface and internal waves," J. Mar. Res. **26**, 208 (1968).

[5] Y. V. Lvov and E. G. Tabak, "Hamiltonian formalism and the Garrett–Munk spectrum of internal waves in the ocean," Phys. Rev. Lett. **87**, 168501 (2001).

[6] C. H. McComas and F. P. Bretherton, "Resonant interaction of oceanic internal waves," J. Geophys. Res. **82**, 1397 (1977).

[7] D. M. Milder, "The effects of truncation on surface-wave Hamiltonian," J. Fluid Mech. **216**, 249 (1990).

[8] P. M. D. J. Olbers, "On the dynamics of internal waves in the deep ocean," J. Geophys. Res. **80**, 3848 (1975).

[9] D. J. Olbers, "On the energy balance of small scale internal waves in the deep sea," Hamburg, Geophys. Einzelschriftern **27** (1974).

[10] D. J. Olbers, "Nonlinear energy transfer and the energy balance of the internal wave field in the deep ocean," J. Fluid Mech. **74**, 375 (1976).

[11] E. N. Pelinovsky and M. A. Raevsky, "Weak turbulence of the internal waves of the ocean," Atm. Ocean Phys.-Izvestija **13**, 187 (1977).

[12] N. Pomphrey, J. D. Meiss, and K. M. Watson, "Description of nonlinear internal wave interactions using Langevin methods," J. Geophys. Res **85**, 1085 (1980).

[13] A. G. Voronovich, "Hamiltonian formalism for internal waves in the ocean," Izvestiya, Atmospheric and Oceanic Physics **15**, 52 (1979).

[14] V. E. Zakharov, V. S. L'vov, and G. Falkovich, *Kolmogorov Spectra of Turbulence I: Wave Turbulence*, Springer-Verlag, Berlin, 1992.

[15] K. Polzin, "A heuristic description of internal wave dynamics," J. Phys. Oceanogr. **34**, 214 (2004).

[16] C. H. McComas and P. Müller, "Time scales of resonant interactions among oceanic internal waves," J. Phys. Oceanogr. **11**, 139 (1981).

[17] Y. V. Lvov, K. L. Polzin, and N. Yokoyama, "Wave-wave interactions in stratified fluids: A comparison of approaches," (submitted to J. Phys. Oceanogr.).

[18] P. G. Müller, G. Holloway, F. Henyey, and N. Pomphrey, "Nonlinear interactions among internal gravity waves," Reviews of geophysics **24**, 493 (1986).

[19] K. L. Polzin, Y. V. Lvov, and E. G. Tabak, "Towards regional characterization of internal wave fields," (in preparation).

[20] P. Müller, D. J. Olbers, and J. Willebrand, "The IWEX spectrum," J. Geophys. Res. **83**, 479 (1978).

[21] M. D. Levine, C. A. Paulson, and J. H. Morison, "Observations of internal gravity waves under the arctic pack ice," J. Geophys. Res. **92**, 779 (1987).

[22] M. D. D'Asaro, E. A. & Morehead, "Internal waves and velocity fine structure in the Arctic Ocean," J. Geophys. Res. **96**, 12725 (1991).

[23] R. A. Weller, K. L. Polzin, D. L. Rundnick, C. C. Eriksen, and N. S. Oakey, "Forced ocean response during the Frontal Air-Sea Interaction Experiment," J. Geophys. Res. **96**, 8611 (1991).

[24] C. Eriksen, D. Rudnick, R. Weller, R. T. Pollard, and L. Regier, "Ocean frontal variability in the Frontal Air-Sea Interaction Experiment," J. Geophys. Res. **96**, 8569 (1991).

[25] J. T. Sherman and R. Pinkel, "Estimates of the vertical wavenumber–frequency spectra of vertical shear and strain," J. Phys. Oceanogr. **21**, 292 (1991).

[26] S. Anderson, *Shear, strain, and thermohaline vertical fine structure in the upper ocean*, PhD thesis, UCSD, 1992.

[27] K. L. Polzin, E. Kunze, J. M. Toole, and R. W. Schmitt, "The partition of finescale energy into internal waves and subinertial motions," J. Phys. Oceanogr. **33**, 234 (2003).

[28] R. A. Weller, P. W. Furey, M. A. Spall, and R. E. Davis, "The large-scale cotext for oceanic subduction in the northeast atlantic," Deep-Sea Res. I **51**, 665 (2004).

[29] R. W. Schmitt, J. R. Ledwell, E. T. Montgomery, K. L. Polzin, and J. M. Toole, "Enhanced diapycnal mixing by salt fingers in the thermocline of the tropical atlantic," Science **308**, 685 (2005).

[30] T. Keffer, "The baroclinic stability of the atlantic north equatorial current," J. Phys. Oceanogr. **13**, 624 (1983).

[31] N. P. Foffonoff, "Spectral characteristics of internal waves in the ocean," Deep Sea Res. *Suppl.* to **16**, 58 (1969).

[32] E. A. D'Asaro, "Wind forced internal waves in the North Pacific and Sargasso Sea," J. Phys. Oceanogr. **14**, 781 (1984).

[33] E. A. D'Asaro, "A collection of papers on the ocean storms experiment," J. Phys. Oceanogr. **25**, 2817 (1995).

[34] Y. V. Lvov, K. L. Polzin, and E. G. Tabak, "Energy spectra of the ocean's internal wave field: theory and observations," Phys. Rev. Lett. **92**, 128501 (2004).

[35] V. E. Zakharov, "Stability of periodic waves of finite amplitude on the surface of a deep fluid," J. Appl. Mech. Tech. Phys. **2**, 190 (1968).

[36] V. E. Zakharov, "The instability of waves in nonlinear dispersive media," Sov. Phys. JETP **24**, 740 (1967).

[37] E. A. Kuznetsov, "On turbulence of ion sound in plasma in a magnetic field," Zh. Eksper. Teoret. Fiz **62**, 584 (1972).

[38] Y. V. Lvov and N. Yokoyama, "Nonlinear wave-wave interactions in stratified flows: Direct numerical simulations," (submitted to Phys. Fluids).

[39] Naturally this condition coincides with (33a).